Development 133, 2671-2681 (2006) doi:10.1242/dev.02439

Coordinated cell-shape changes control epithelial movement in zebrafish and *Drosophila*

Mathias Köppen[1], Beatriz García Fernández[2], Lara Carvalho[1], Antonio Jacinto[2] and Carl-Philipp Heisenberg[1,*]

Epithelial morphogenesis depends on coordinated changes in cell shape, a process that is still poorly understood. During zebrafish epiboly and *Drosophila* dorsal closure, cell-shape changes at the epithelial margin are of critical importance. Here evidence is provided for a conserved mechanism of local actin and myosin 2 recruitment during theses events. It was found that during epiboly of the zebrafish embryo, the movement of the outer epithelium (enveloping layer) over the yolk cell surface involves the constriction of marginal cells. This process depends on the recruitment of actin and myosin 2 within the yolk cytoplasm along the margin of the enveloping layer. Actin and myosin 2 recruitment within the yolk cytoplasm requires the Ste20-like kinase Msn1, an orthologue of *Drosophila* Misshapen. Similarly, in *Drosophila*, actin and myosin 2 localization and cell constriction at the margin of the epidermis mediate dorsal closure and are controlled by Misshapen. Thus, this study has characterized a conserved mechanism underlying coordinated cell-shape changes during epithelial morphogenesis.

KEY WORDS: Zebrafish epiboly, *Drosophila* dorsal closure, Cell shape, *Misshapen*, Actin, Myosin 2

INTRODUCTION

Contraction of an epithelial sheet to close an opening is a common process in animal development and tissue repair, and requires extensive modification of cell shape at the advancing epithelial margin (Martin and Parkhurst, 2004). Many of the cellular and molecular mechanisms controlling this event have been identified by analysis of *Drosophila* dorsal closure (reviewed by Harden, 2002; Jacinto et al., 2002b). Dorsal closure is one of the last morphogenetic movements during *Drosophila* embryogenesis and occurs as the opposing fronts of the lateral epidermis converge dorsally, displacing the underlying amnioserosa (Martinez-Arias, 1993). A central aspect of this process is the uniform elongation and constriction of marginal epidermal cells. This transforms the margin from a loose, scalloped edge into a taut row of cells and probably ensures even epithelial advance (Jacinto et al., 2002a; Young et al., 1993). The observed accumulation of actin and myosin 2 in these cells suggests that the transformation of the margin is achieved by a contractile actomyosin 'cable'. However, to what extent this represents a general mechanism controlling epithelial movement is unclear.

Similar to the *Drosophila* epidermis, the outer epithelium of the zebrafish embryo, the enveloping layer (EVL), is a simple epithelium that spreads over the spherical yolk cell together with the underlying deep cells, to ultimately seal the embryo on the vegetal side (Kane and Adams, 2002; Kimmel et al., 1995) (for illustration, see Fig. 1L). During EVL epiboly, the length of the advancing margin must be reduced as the tissue closes around the vegetal yolk blastopore. Analysis of the related teleost *Fundulus heteroclitus* has shown that this involves the constriction of marginal EVL cells (Keller and Trinkaus, 1987), similar to *Drosophila* dorsal closure. However, the mechanistic basis for EVL cell shape change remains to be shown.

Insights come from studies of both *Fundulus* and zebrafish, and suggest a potential role of the underlying yolk syncytial layer (YSL) during EVL epiboly. The YSL constitutes the surface of the yolk cell directly beneath the blastoderm and undergoes epiboly simultaneously with the EVL. In *Fundulus*, the leading edges of marginal EVL cells were found to be stably attached to the YSL while undergoing constriction. Furthermore, a dense network of microfilaments was detected in the YSL along the EVL margin in *Fundulus* (Betchaku and Trinkaus, 1978; Keller and Trinkaus, 1987). A similar accumulation of actin within the YSL has recently also been reported in zebrafish, and was implicated in EVL epiboly (Cheng et al., 2004). This suggests that the YSL may control changes in marginal EVL cell shape via an actin-dependent mechanism. However, YSL-specific analysis supporting a role for actin during EVL epiboly has so far been missing. Furthermore, the molecular mechanisms controlling actin function in the YSL are still unknown.

In this study, we show that localized recruitment of actin and myosin 2 within the YSL correlates with EVL cell-shape change. Furthermore, we show that this process is dependent on Msn1, a zebrafish ortholog of the *Drosophila* Ste20-like kinase Misshapen. Similarly, we show that *Drosophila* Misshapen is required for actin/myosin 2-based cell constriction at the epidermal margin during dorsal closure. These findings point to a conserved mechanism of actin/myosin 2 recruitment and cell constriction during epithelial morphogenesis in zebrafish and *Drosophila*.

MATERIALS AND METHODS

Zebrafish embryo maintenance

All embryos were obtained from zebrafish AB, TL and Wik wild-type lines, grown at 31°C, and manipulated in E3 zebrafish embryo medium or Danieau buffer.

Drosophila stocks and genetic crosses

Wild-type embryos were from the Oregon R strain. UAS lines were expressed using the Gal4 system (Brand and Perrimon, 1993). The Gal4 lines *e22c-Gal4*, *LE-Gal4*, *en-Gal4* (Brand and Perrimon, 1993), and *c381-Gal4 (AS-Gal4)* and flies carrying the GFP balancer *TM3*, *gal4-twi*, *UAS-2xEGFP (TTG)* were kindly provided by the Bloomington stock centre. msn^{172} was kindly provided by J. Treisman. Homozygous msn^{172} embryos

[1]Max Planck Institute of Molecular Cell Biology and Genetics, Pfotenhauerstr.108, 01307 Dresden, Germany. [2]Instituto de Medicina Molecular, Edificio Egas Moniz, Av. Profesor Egas Moniz, 1649-028 Lisbon, Portugal.

*Author for correspondence (e-mail: heisenberg@mpi-cbg.de)

Accepted 9 May 2006

expressing GFP-Actin in the *engrailed* domains were generated by crossing *UAS-GFP-Actin/Cyo*; msn^{172}/*TTG* flies to *en-Gal4*; msn^{172}/*TTG* flies. A strain carrying a *UAS-DN-msn* construct was a gift from Yong Rao (Houalla et al., 2005). Homozygous *UAS-DN-msn* flies were crossed with *e22c-Gal4*, *LE-Gal4* or *AS-Gal4* flies to express *DN-msn* in the whole epidermis, marginal cells of the epidermis, or the amnioserosa, respectively.

Identification of *msn* genes and phylogenetic analysis

misshapen-type genes were identified in the zebrafish genome using BLAST analysis. cDNA sequences were obtained from PubMed. Multiple alignments of predicted protein sequences were done using ClustalX (Chenna et al., 2003). Phylogenetic analysis was done using protdist and fitch from the Phylip package [Felsenstein, J. 1989. PHYLIP (Version 3.2). Cladistics 5: 164-166]. The phylogenetic tree was displayed using NJplot (Perriere and Gouy, 1996).

RNA in situ hybridization

In situ staining of zebrafish embryos were performed as previously described (Barth and Wilson, 1995). In situ probes were synthesized from cDNA using a DIG RNA labeling kit (Roche). The msn1 in situ probe corresponded to bases 1230-2341 of the msn1 cDNA sequence (PubMed Accession number AAH55134.1).

Morpholino injections of zebrafish embryos

The following morpholino oligonucleotides (MOs) (Heasman, 2002) were used: *msn1MO-splice* (5′-ACACACAACTTACccttaaagtgga-3′); *msn1MO-splice5bp* (5′-ACACAGAAGTTACCGTTAAACTGCA-3′), *msn1MO-ORF* (5′-CTCGCCATATTAAAGACGAAAAAAC-3′, *msn1MO-UTR* (5′-GAATAGACCTCTCAGTCAGTCGTCC-3′), *msn2-ORF* (5′-GCGGGA-GAGTCGTTCGCCATCTTTC-3′), *msn3-ORF* (5′-TGCGTTTTCTGAC-ATTTTCACAACG-3′), *e-cadMO* (5′-ATCCCACAGTTGTTACACAA-GCCAT-3′). Embryos were injected at the one-cell stage as previously described (Barth and Wilson, 1995). YSL injection was performed at the sphere stage. For rescue of msn1MO phenotypes, 200 pg of full-length *msn1* mRNA (PubMed Accession number AAH55134.1) and 2 ng of *msn1MO-splice* were injected into the YSL. Effective YSL-injection was monitored by co-injecting Alexa 488 Histone H1 (Molecular Probes), which labels YSL nuclei (D'Amico and Cooper, 2001).

RT-PCR analysis

Total RNA was purified from zebrafish embryos using Trizol reagent (Invitrogen). mRNA was then purified using PolyAtract reagents (Promega). cDNAs were generated using the SMART RACE cDNA Amplification Kit (Clontech). The *msn1* splicing pattern was analyzed by PCR amplification using the primers P1 (5′-TGTACCAGAAGCAAGAGCGAGC-3′) and P2 (5′-CATCCATGCACTTGATAGCAGCC-3′).

Drosophila cuticle preparations

Embryos were collected on yeasted apple juice agar plates for 24 h and aged for 48 h at 25°C. They were then dechorionated in bleach, rinsed in water, mounted in a 1:1 mixture of acetic acid and Hoyer's medium, and incubated for 12 h at 65°C.

Antibody and phalloidin staining

Zebrafish embryos were fixed overnight in 2% or 4% paraformadehyde at 4°C, then washed in 0.1% Triton in PBS (PBT) and dechorionated. They were then incubated for 1 h in 0.5% Triton in PBS, followed by a 5-h incubation in block solution (10% normal goat serum, 1% DMSO, 0.1% Triton in PBS). Embryos were then incubated overnight at 4°C in block solution containing Phalloidin and/or primary antibodies. They were then washed in PBT, and incubated for 5 h at room temperature with secondary antibodies. Antibody and Phalloidin staining of *Drosophila* embryos were performed as previously described (Kaltschmidt et al., 2002). Alexa 488 Phalloidin and Alexa 594 Phalloidin (Molecular Probes) were used at 1:200 dilutions. The following primary antibodies and dilutions were used: rabbit anti-E-cadherin at 1:750 (Babb et al., 2001), rabbit anti-α-catenin and mouse anti-β-catenin at 1:500 (Sigma), mouse anti-ZO-1 (a gift from S. Tsukita) at 1:25, rabbit anti-Claudin-1 at 1:400 (Zymed), rabbit anti-phospho-myosin light chain 2 Ser19 (Cell Signalling) at 1:100, rabbit anti-Msn at 1:50 (Houalla et al., 2005), rabbit anti-myosin 2 at 1:500 (Kiehart and Feghali, 1986), and mouse anti-Armadillo at 1:50 (Developmental Studies Hybridoma Bank, ref. N2 7A1). Zebrafish embryos were mounted on agarose-coated dishes in PBT medium, *Drosophila* embryos were mounted in Vectashield (Vectorlabs). Images were acquired on a Zeiss LSM and a Leica TCS-SP2 confocal microscope.

Live imaging

Time-lapse, multiple focal plane (4D) microscopy of zebrafish embryos expressing GAP-43-GFP and cytosolic GFP was performed as previously described (Montero et al., 2005). Live imaging of *Drosophila* embryos was performed as previously described (Jacinto et al., 2000).

Drug treatments

Dechorionated zebrafish embryos were incubated in 50 μm (±)-blebbistatin or (+)-blebbistatin (Calbiochem) after the 50% epiboly stage, and were compared to control embryos in Danieau buffer; 4 ng of *e-cadMO* was injected into one-cell-stage embryos, which were then incubated in blebbistatin after 50% epiboly.

Electron microscopy

Embryos were fixed in 4% paraformaldehyde, 2% glutaraldehyde in 0.1 M phosphate buffer overnight, then postfixed in 1% osmium tetroxide (Science Services) for 1 h, dehydrated through a graded series of ethanol, and infiltrated in Embed-812 resin (Science Services) overnight. Samples were cured for 48 h at 65°C. Ultrathin sections (70 nm thick) were cut on an Ultracut microtome (Leica Microsystems). Samples were viewed in a Morgagni EM (FEI).

Quantification of cell shape and actin localization

Images of Phalloidin-stained zebrafish embryos were analyzed using ImageJ software (http://rsb.info.nih.gov/ij/). The length of marginal EVL cells was defined as the distance between the middle of the leading edge of the cell and the animal-most region of the cell. Cell width was defined as the distance between the centers of the lateral cell boundaries of a cell. Length/width ratio of a cell was correlated with the local Phalloidin density in the adjacent YSL. Phalloidin density was defined as the average pixel intensity within a rectangle immediately adjacent to the leading edge of the cell. Data presented were based on one experiment. Repeats of the experiment yielded similar results. Phalloidin signal intensity profiles were generated by plotting pixel intensity along a line from the EVL margin towards the vegetal pole. Several profiles were generated for each embryo. Average profiles of multiple embryos are shown.

PubMed Accession Numbers of protein sequences used in the phylogenetic analysis

Drosophila Misshapen: NP_524679.2
Zebrafish Msn1: AAH55134.1
Zebrafish Msn2: fj33a09 (EST)
Zebrafish Msn3: AL921244
Human TRAF2 and NCK interacting kinase (Traf2_NCK): Q9UKE5
Human MAP4 kinase 4: O95819
Human MAP4 kinase 6: NP_733763.1
Mouse Traf2_NCK: XP_130797.3
Mouse MAP4 kinase 4: P97820
Mouse MAP4 kinase 6: NP_795712.1
C. elegans Mig-15: NP_509747.1

RESULTS

Actin and myosin 2 accumulation in the YSL correlates with EVL cell-shape changes during zebrafish epiboly

Previous analysis indicated a potential role of the actin cytoskeleton within the YSL for EVL epiboly (Cheng et al., 2004). We therefore addressed how actin distribution in the YSL relates to the morphology and arrangement of EVL cells during epiboly (for illustration of tissue organization during epiboly, see Fig. 1L). To visualize actin distribution in addition to outlining the EVL cells, we

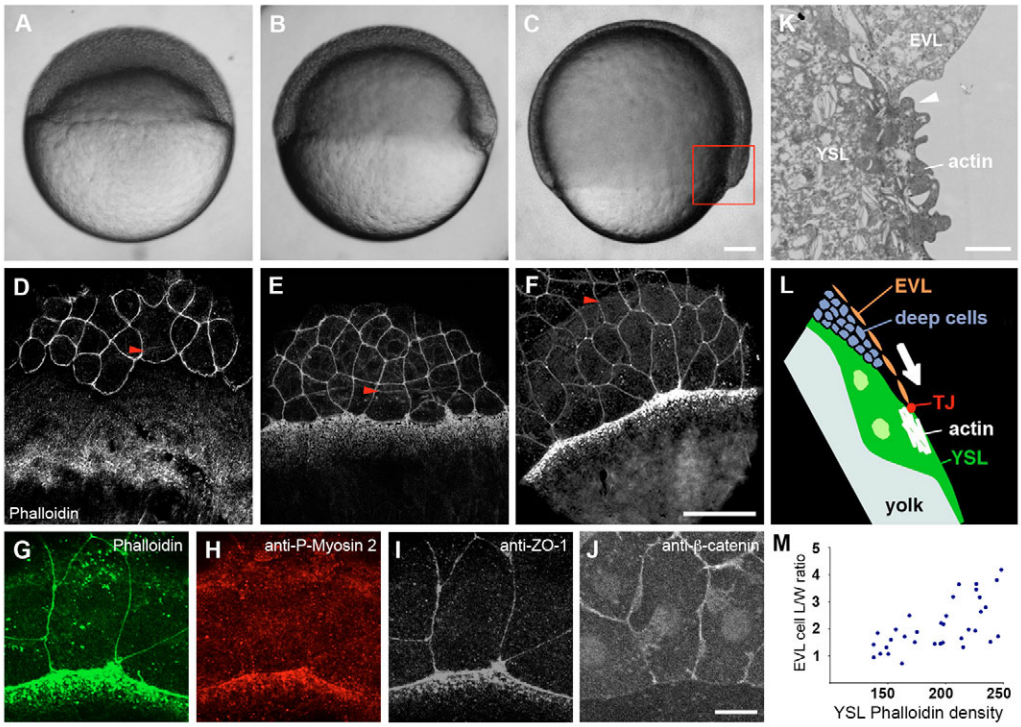

Fig. 1. Actin, myosin 2 and ZO-1 become enriched at the EVL-YSL interface. (**A-F**) Wild-type embryos at dome (A,D), shield (B,E) and 75% epiboly stages (C,F) as bright-field images (A-C) and stained with Phalloidin (F-actin) (D-F). Arrowheads indicate the position of the advancing margin of the deep cells. All zebrafish embryos in these and subsequent panels are displayed with the animal pole at the top unless otherwise indicated. (**G-J**) Co-staining of the EVL-YSL interface at 75% epiboly with Phalloidin and antibodies against phospho-myosin light chain 2 and ZO-1 (G-I), and single-staining against β-catenin (J). (**K**) Transmission electron microscopy image of a cross-section through the EVL and YSL at 75% epiboly. Arrowhead points at the EVL-YSL contact. (**L**) Schematic representation of the boxed region in C, showing the basic organization of the embryonic cell layers. The blastoderm consists of the EVL and deep cell layers and is in contact with the underlying YSL, the surface of the yolk cell. The arrow indicates the movement direction of the blastoderm during epiboly. (**M**) Relationship between the length/width ratio of individual marginal EVL cells and local Phalloidin signal intensity in the adjacent YSL at 75% epiboly. The values of 34 cells from 6 embryos were plotted. Abbreviations: EVL, enveloping layer; TJ, tight junction; YSL, yolk syncytial layer. Scale bars: in C, 100 μm for A-C; in F, 50 μm for D-F; in J, 25 μm for G-J; in K, 2 μm.

stained embryos with fluorescently labeled Phalloidin at different epiboly stages. Throughout this study, epiboly stages reflect the position of the margin of the deep cell layer.

At 30% epiboly, the EVL margin had advanced towards the vegetal pole to the same extent as the underlying deep cells. Marginal EVL cells were oval shaped and loosely aligned. A diffuse band of actin was present at the YSL cortex in the vicinity of the EVL margin (Fig. 1A,D). At the onset of mesendoderm ingression, actin within the YSL became sharply concentrated along the EVL margin. Simultaneously, the marginal EVL cells were aligned along the equator, and typically displayed a rectangular shape (Fig. 1B,E). At 75% epiboly, the EVL margin was positioned clearly ahead of the deep cells. A dense ring of actin had formed within the YSL along the EVL margin, and the majority of EVL cells were clearly elongated in the movement direction (Fig. 1C,F).

We noticed that at 75% epiboly, both actin concentration in the YSL and marginal EVL cell shape had become increasingly variable. Interestingly, we found a direct correlation between the length/width ratio of individual marginal EVL cells and the amount of actin in the adjacent YSL (Fig. 1M, see Materials and methods). This suggests that local recruitment of actin in the YSL is linked to the elongation and narrowing of EVL cells that occurs as the epithelium advances towards the vegetal pole.

Given the evidence from *Drosophila* that actin/myosin 2-based contraction occurs at the leading edge of the epidermis during dorsal closure, we looked for myosin 2 in the zebrafish YSL by staining embryos with an antibody against phosphorylated (activated) myosin light chain 2. Weak staining was detected at the boundaries between EVL cells, and at late stages of epiboly, the signal became enriched within the YSL along the EVL margin, similar to the Phalloidin signal (Fig. 1G,H). Thus, both actin and myosin 2 reside within the YSL in the direct vicinity of marginal EVL cells as these cells undergo dynamic changes in shape.

In *Fundulus*, EVL cells at the margin appear to be connected to the YSL via tight junctions (Betchaku and Trinkaus, 1978). To characterize this linkage in zebrafish, we first analyzed zebrafish embryos at 75% epiboly using transmission electron microscopy. We detected structures at the EVL-to-YSL interface that resemble tight junctions but not adherens junctions (Fig. 1K). Consistent with this, antibodies against zebrafish ZO-1 (Fig. 1I) and human Claudin-1 (data not shown), both known components of vertebrate tight junctions (D'Atri and Citi, 2002), predominantly labeled the leading edges of marginal EVL cells, and the immediately adjacent YSL. In addition, both markers labeled the boundaries between EVL cells. In contrast, antibodies against E-cadherin, α-catenin and β-catenin, components of adherens junctions (Nagafuchi, 2001), strongly labeled the borders between EVL cells, but only very weakly labeled

the EVL-to-YSL interface (Fig. 1J, and data not shown), indicating that the linkage between these tissues does not primarily involve adherens junctions.

Together, these results suggest that actin and phospho-myosin light chain 2 recruitment within the YSL to the EVL margin and the physical linkage between both tissues via tight junctions are involved in controlling cell constrictions at the EVL margin.

Identification of zebrafish *misshapen* orthologs

The *Drosophila* MAP4 kinase Misshapen and its orthologs in other organisms have been implicated in the control of actin-based cell movement, including *Drosophila* dorsal closure (Ruan et al., 2002; Ruan et al., 1999; Su et al., 1998; Su et al., 2000; Xue et al., 2001). We therefore determined the specific requirement for Misshapen-type molecules in actin-based cell constriction both during EVL epiboly in zebrafish and *Drosophila* dorsal closure.

To address a potential role of Misshapen-like proteins during zebrafish epiboly, we first identified orthologues of *Drosophila misshapen* in the zebrafish genome. We identified three genes (*msn1-3*) encoding MAP4 kinase proteins with high similarity to *Drosophila* Misshapen. Phylogenetic analysis suggests that Msn1-3 each clearly group with one of the three Misshapen-related proteins in mammals (Fig. 2A).

To assess potential functions of these genes during zebrafish epiboly, we performed gene 'knock-down' experiments by injecting specific morpholino-oligonucleotides (MOs) targeting the coding region of each gene into one-cell stage embryos. *msn1* MOs caused clear defects during gastrulation (described below). Weaker gastrulation defects were observed in the case of an *msn2* MO, while no defects were observed in the case of an *msn3* MO (data not shown). We co-injected MOs against *msn1* and *msn2*, but no obvious enhancement of the *msn1* morphant phenotype was observed (data not shown). This suggests that both genes function non-redundantly. For the remainder of this study, we focus specifically on *msn1* function.

Comparison of the predicted protein sequences of *Drosophila* Misshapen and Msn1 revealed 77% identity of the N-terminal kinase domain, and 73% identity of the C-terminal CNH (citron homology) domain (Fig. 2B).

To characterize the RNA expression pattern of *msn1* during embryogenesis, we performed whole-mount in situ hybridization using a probe against the non-conserved central domain of the message. *msn1* was detected at early cell division stages (Fig. 2C), and is therefore maternally provided. At shield and bud stages, we detected weak, ubiquitous expression throughout the embryo (Fig. 2D,E).

msn1 is required for gastrulation movements

To address the role of *msn1* during gastrulation, we injected 1-8 ng of three independent *msn1*-specific MOs at the one-cell stage, and observed similar embryonic defects in each case. The splicing morpholino *msn1MO-splice* was used for the phenotypic analysis presented in this study. A quantification of the effects of the other MOs is included in our description of YSL-specific MO injections below.

msn1MO-splice targets the exon 1/intron 1 boundary of the pre-mRNA. Sequence analysis of the *msn1* mRNA of embryos injected with this MO revealed changes in the splicing pattern, that eliminate the exon sequence encoding amino acids 1-19 of the predicted protein (see Fig. S1A in the supplementary material). Usage of a potential alternative start codon (encoding amino acid 56) would truncate the N-terminal Ser/Thr kinase domain (amino acids 25-289). This suggests that *msn1MO-splice* probably interferes significantly with *msn1* function, but may not lead to complete protein loss.

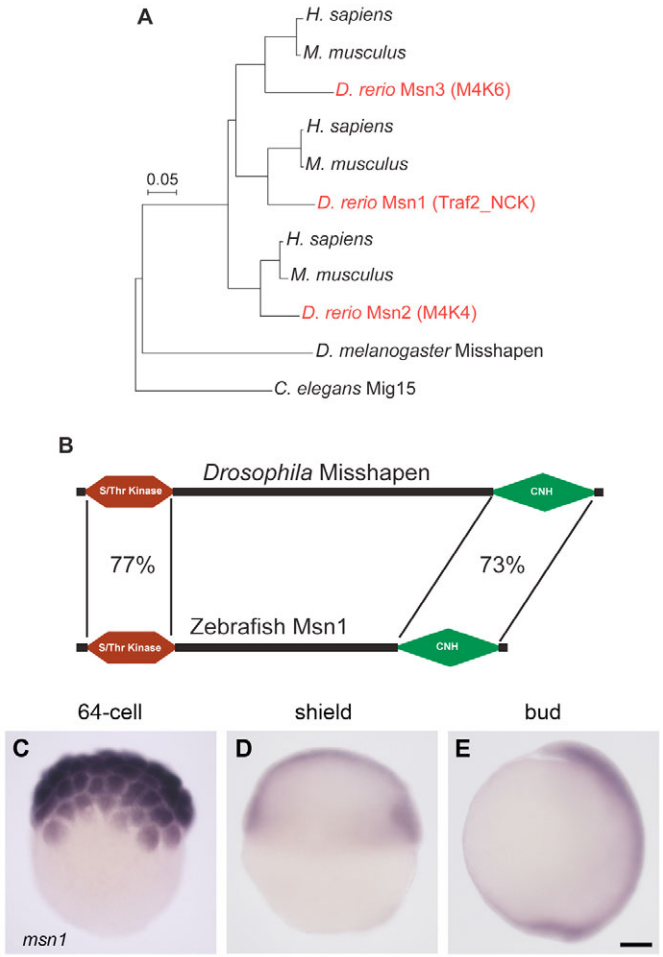

Fig. 2. *msn1* encodes a zebrafish orthologue of *Drosophila* Misshapen and is expressed during gastrulation. (**A**) Phylogenetic analysis of zebrafish homologues (Msn1-3) of *Drosophila* Misshapen. The scale bar indicates point mutations per site. Msn1 is most closely related to human and mouse Traf2_NCK (Traf2 and NCK interacting kinase). (**B**) Protein domain comparison of zebrafish Msn1 and *Drosophila* Misshapen. Percentage amino acid identity between conserved N-terminal Ser/Thr kinase and C-terminal CNH (citron homology) domains is indicated. (**C-E**) *msn1* mRNA expression during early cell division gastrulation stages. In situ hybridization of wild-type embryos at 64-cell (C), shield (D) and bud stages (E). Dorsal is to the right in D and E. Scale bar in E: 100 μm for C-E.

Morphant embryos appeared morphologically normal and displayed no obvious defects in patterning at shield stage (see Fig. S1B-E in the supplementary material). However, during subsequent stages, we observed epiboly defects in 65% of the embryos. In addition, defects in the convergence and extension of the main body axis were frequently observed (see Fig. S1F-L in the supplementary material). This suggests that *msn1* is required for the process of epiboly as well as for convergence and extension movements.

msn1 is required in the YSL for actin and myosin 2 recruitment and EVL cell-shape changes

The above results suggest a function of *msn1* in multiple gastrulation movements. However, since these movements are probably interdependent, the specific role of *msn1* during EVL/YSL epiboly remained unclear. We therefore directly

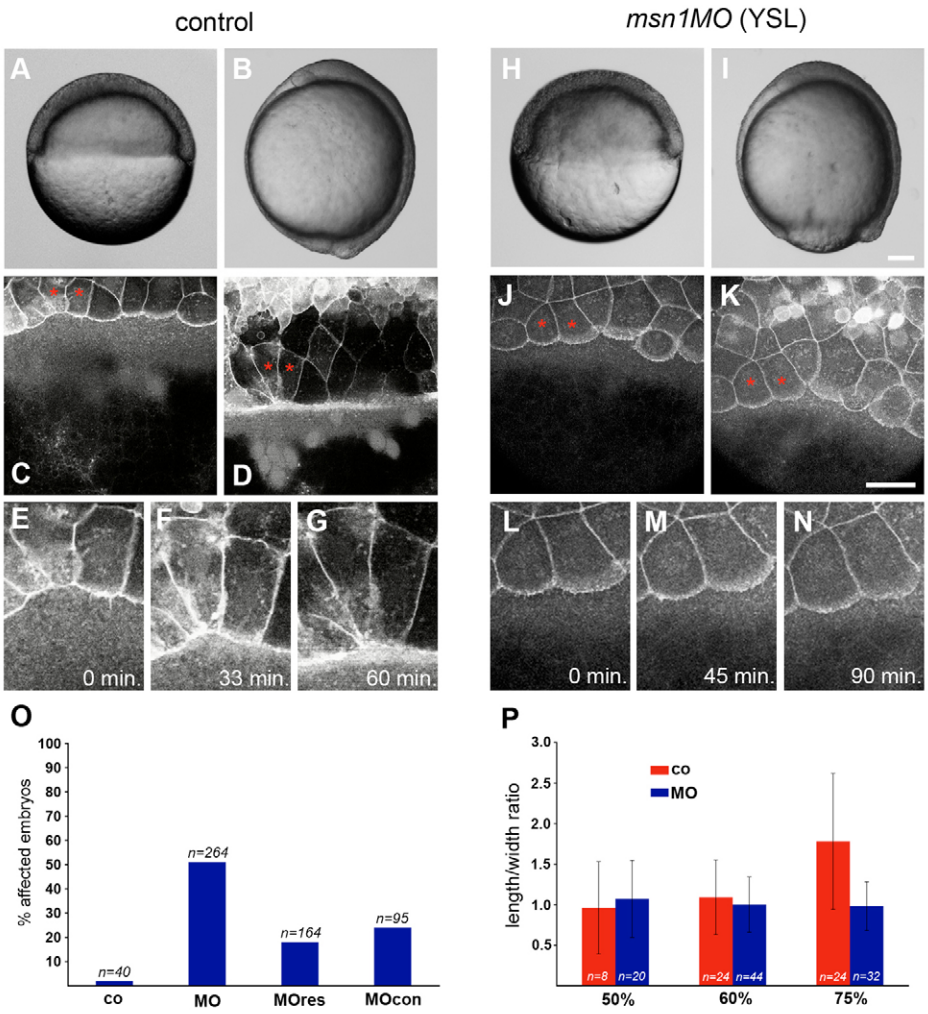

Fig. 3. *msn1* is required in the YSL for dynamic cell-shape changes of the EVL during epiboly. In this and subsequent figures, zebrafish embryos of the same age are compared unless otherwise stated. (**A**,**B**,**H**,**I**) Bright-field images of control and YSL-*msn1*-morphant embryos at 50% epiboly (A,H) and bud stage (B,I). Dorsal is to the right. (**C**,**D**,**J**,**K**) Images from multi-photon time-lapse analysis of EVL epiboly. The EVL plasma membrane was labeled with GAP-43-GFP. Control and YSL-morphant embryos are shown at 50% epiboly (C,J) and after the EVL margin had advanced approx. 100 μm (D,K). (**E-G**,**L-N**) Magnified views of the cells labeled with asterisks in (C,D,J,K). Control (E-G) and morphant cells (L-N) are shown at 50% epiboly (0 min) and at the indicated timepoints. (**O**) Quantification of epiboly defects resulting from various YSL morpholino injections. Shown are the percentages of embryos displaying delayed epiboly (80-95% epiboly) when uninjected embryos had reached the 100% epiboly stage. Abbreviations: co, control; MO, *msn1MO-splice*; MOres, *msn1MO-splice* + *msn1* RNA; MOcon, *msn1MO-splice5bp*. Numbers are based on three independent experiments. (**P**) Mean and standard deviation of the length/width ratio of cells at the EVL margin in control and morphant embryos at 50%, 60% and 75% epiboly. Scale bars: in I, 100 μm for A,B,H,I ; in K, 50 μm for C-G,J-N.

addressed the role of *msn1* in the YSL by injecting morpholinos into this tissue prior to the onset of epiboly. Embryos injected with 8 ng *msn1MO-splice* displayed no obvious abnormalities until 50% epiboly (approximately 75 min after injection, Fig. 3A,H), after which half of the embryos showed a delay in epiboly of the deep cell layer and the EVL, while convergence and extension occurred at the normal rate (Fig. 3B,I,O). The deep cell epiboly delay probably occurred as a secondary consequence of impaired EVL epiboly, as the EVL margin limits how far deep cells can progress towards the vegetal pole.

The observed phenotypes are most likely to be due to a reduction of *msn1* function in the YSL, since co-injection of wild-type *msn1* mRNA into the YSL suppressed the epiboly defect to a large extent, and the injection of a 5-base-mispair MO (*msn1MO-splice5bp*) caused a significantly less-penetrant phenotype (Fig. 3O). Furthermore, YSL injection of two additional MOs caused similar phenotypes: 1 ng of *msn1MO-ORF* (targeting the open reading frame) resulted in a clear delay of epiboly in 79% of the embryos (n=70), while injection of 8 ng of *msn1MO-UTR* (targeting the 5′UTR) caused epiboly delay in 24% of the embryos (n=74).

To specifically identify the role of *msn1* in the YSL for EVL epiboly, we analyzed morphant embryos with respect to three main aspects: (1) EVL cell shape, (2) localization of actin and myosin 2 in the YSL, and (3) the linkage between EVL and YSL. We analyzed changes in EVL cell shape between 50% and 75% epiboly both in live embryos, using multi-photon confocal microscopy, and in Phalloidin-stained embryos. At 50% epiboly, marginal cells of control embryos were typically oval shaped and displayed protrusive activity at their leading edges. Shortly after, protrusive activity ceased, and during subsequent stages the average length/width ratio of marginal cells increased, reflecting the elongation and narrowing of these cells. In addition, cell shapes at the margin became increasingly variable, as some cells underwent leading edge constriction while adjacent cells became wider. Frequently, the collapse of the leading edge of cells resulted in the elimination of these cell from the margin (Fig. 3C-G,P; see Movie 1 in the supplementary material). Morphant embryos showed normal cell morphology at 50% epiboly, but failed to undergo the later changes observed in the controls. The rate of margin progression towards the vegetal pole was slowed, the average the length/width ratio remained essentially constant, and little variability in cell shape was observed at 75% epiboly (Fig. 3J-N,P; see Movie 2 in the supplementary material).

To address whether these cell-shape defects correlated with impaired recruitment of actin and myosin 2 in the YSL, we co-stained embryos with Phalloidin and the phospho-myosin 2 antibody. At 50% epiboly, diffuse Phalloidin signal was observed in the YSL of control and morphant embryos (Fig. 4A,B). In control embryos, the Phalloidin and anti-phospho myosin 2 signals became markedly enriched within the YSL along the EVL margin as the embryos reached 75% epiboly (Fig. 4C,E,G). In morphant embryos, this enrichment of both markers was clearly weaker (Fig. 4D,F,H).

To address whether reducing *msn1* function in the YSL interferes with the formation of tight junctions between EVL and YSL, we stained morphant embryos with the anti-ZO-1 antibody. No clear abnormalities in the staining pattern were observed (data not shown), arguing against a defect in tight junction formation in these embryos.

The above results indicate that *msn1* is required in the YSL for the recruitment of actin and myosin 2 and for cell-shape changes of marginal EVL cells.

Myosin 2 is required for effective actin accumulation and EVL progression during epiboly

The above results show that actin and myosin 2 recruitment correlates with the progression of EVL/YSL epiboly. To directly address the role of actin/myosin 2 contraction in the YSL, we tested myosin 2 function during EVL/YSL epiboly using the specific myosin 2 inhibitor blebbistatin (Straight et al., 2003).

We found that embryos exposed to (±)-blebbistatin at the onset of gastrulation epibolized at a slower rate than control embryos, typically completing the process with significant delay, or arresting prior to its completion. In contrast, other aspects of gastrulation were only very mildly affected, resulting in the formation of a largely normal body axis. Embryos treated with an inactive form of the drug, (+)-blebbistatin, showed no significant developmental defects (Fig. 5A-C). This suggests that epiboly is directly impaired by blebbistatin.

Next, we analyzed EVL cell shape and actin distribution in blebbistatin-treated embryos during late stages of epiboly. We found that the EVL margin of treated embryos had progressed significantly less towards the vegetal pole compared to untreated embryos. In addition, we noted unusually wide marginal EVL cells, and found that the level of actin accumulation in the YSL along the margin was markedly reduced (Fig. 5D,E). These findings suggest that blebbistatin inhibition of myosin 2 partially impairs actin accumulation in the YSL and slows EVL progression towards the vegetal pole.

To address whether the effect of blebbistatin on EVL epiboly may be caused indirectly through an effect of the drug on deep cell epiboly, we tested whether EVL epiboly is generally dependent on the deep cells. Consistent with previous findings, we observed that the EVL advanced at a normal rate when we severley impaired deep cell epiboly through morpholino-based inactivation of *half baked*/E-cadherin in the embryo (Fig. 5F,G) (Kane et al., 1996; Kane et al., 2005). This suggests that EVL epiboly is independent of the deep cells and is directly inhibited by blebbistatin. In addition, we performed blebbistatin treament of *half baked*/E-cadherin morphants, which enabled us to better visualize and quantify the overall effect of the drug on the EVL. Morphant embryos with or without drug treatment showed a similar delay of deep cell epiboly 9 h after fertilization. However, in the case of no drug treatment, the EVL margin had almost reached the vegetal pole and was positioned 186±9 μm (mean±s.e.m., n=10) ahead of the deep cell margin (Fig. 5F,G), while in drug-treated embryos, the EVL margin had progressed only 71±6 μm (mean±s.e.m., n=11) ahead of the deep cells.

Drosophila Misshapen is required for epidermal cell constriction during dorsal closure

Given the apparent role of cell constriction at the margin both during EVL epiboly in zebrafish and dorsal closure in *Drosophila*, we investigated whether Misshapen may play a similar role during

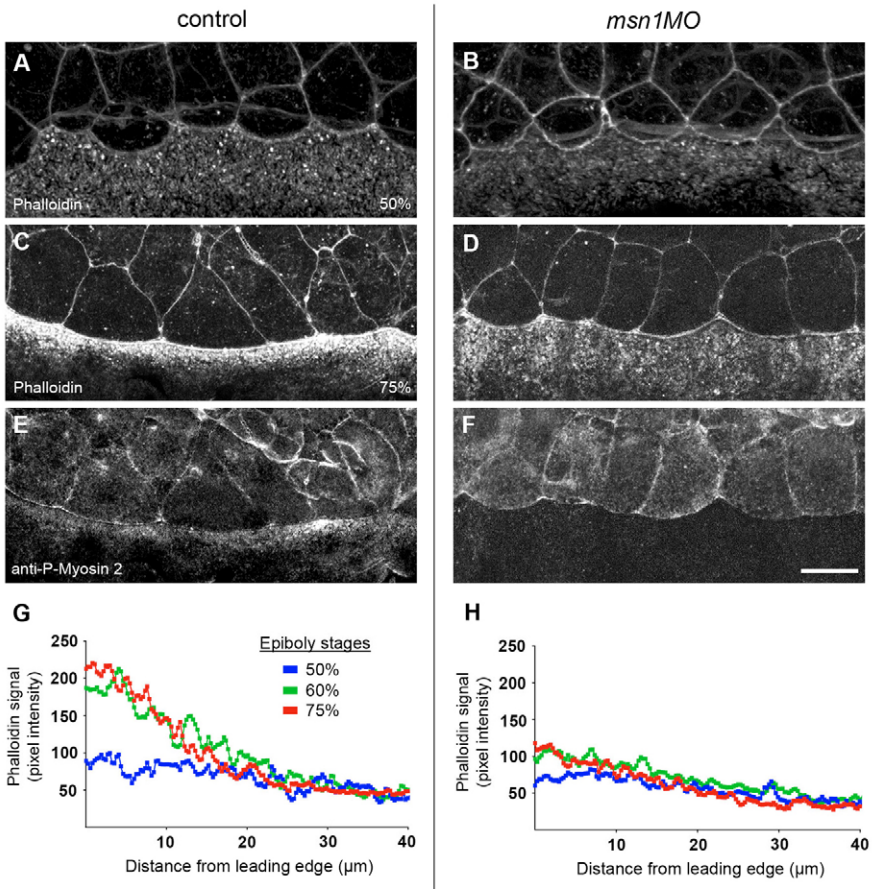

Fig. 4. Cell-shape changes of the EVL during epiboly correlate with *msn1*-mediated recruitment of actin and myosin 2 in the YSL. (**A-F**) Analysis of actin and myosin 2 localization in control and YSL-morphant embryos. Phalloidin staining of embryos at 50% epiboly (A,B) and co-staining of 75% epiboly embryos with Phalloidin and an anti-phospho-myosin light chain 2 antibody (C-F). (**G**,**H**) Intensity profiles of Phalloidin in the YSL in the vicinity of the EVL margin in control (G) and YSL-morphant embryos (H) at 50%, 60%, and 75% epiboly stages. The intensity of the Phalloidin signal was plotted along a line perpendicular to the EVL margin (see Materials and methods). Average plots are shown. Scale bar in F: 25 μm for A-F.

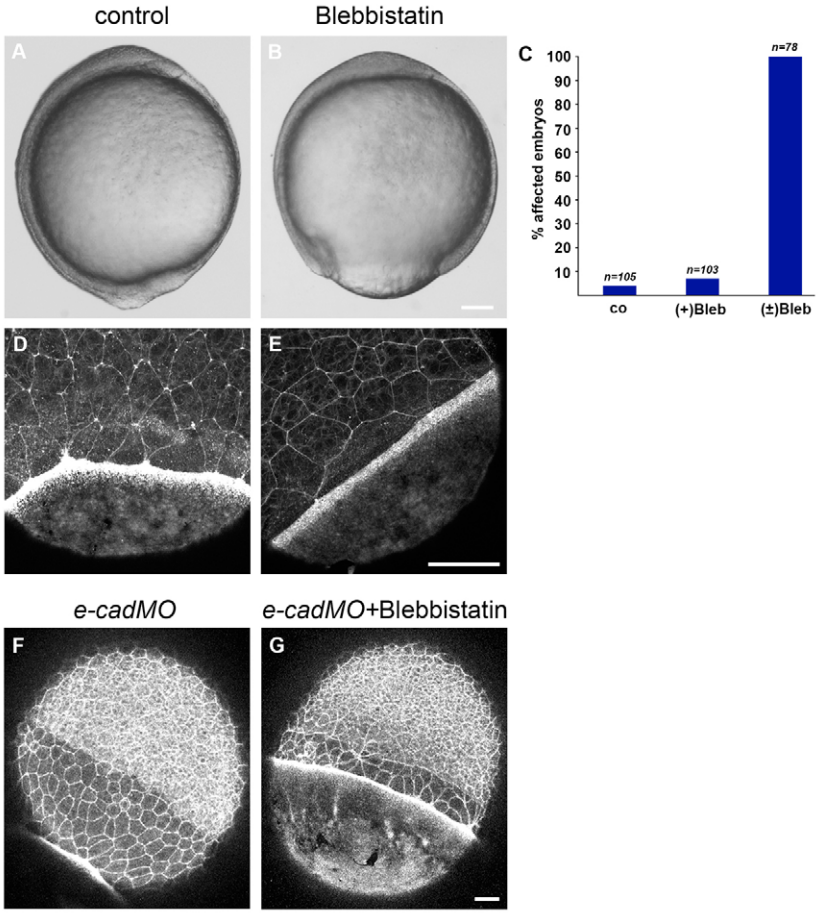

Fig. 5. Treatment with the myosin 2 inhibitor blebbistatin decreases actin recruitment in the YSL and slows the rate of EVL epiboly. (**A**,**B**) Bright-field image of an untreated embryo at bud stage (A) and a (±)-blebbistatin-treated embryo (B). (**C**) Quantification of epiboly defects resulting from blebbistatin treatments. Shown are the percentages of embryos displaying delayed epiboly (80-95% epiboly) when untreated embryos had reached the 100% epiboly stage. Numbers are based on two independent experiments. Abbreviations: co, untreated control; (+)Blb, (+)-blebbistatin treatment; (±)Blb, (±)-blebbistatin treatment. (**D**,**E**) Phalloidin (F-actin) staining of a control embryo at 75% epiboly and a (±)-blebbistatin-treated embryo. (**F**,**G**) Phalloidin staining of an untreated embryo at 90% epiboly (F) and (±)-blebbistatin-treated embryo (G), both injected with a morpholino against *half baked*/E-cadherin. Scale bars: in B, 100 μm for A,B; in E, 50 μm for D,E; in G, 25 μm for F,G.

Drosophila dorsal closure. Consistent with such a role, we found that Misshapen is localized to the cortex of cells of the epidermis and cells of the underlying amnioserosa throughout dorsal closure (Fig. 6A,B).

To characterize the role of Misshapen during dorsal closure, we first determined the range of embryonic defects in embryos homozygous for msn^{172}, a likely null allele of *misshapen* (Treisman et al., 1997). Based on the preparation of cuticles, 2% of mutant embryos displayed an anterior dorsal hole; 38% had closed but showed misalignment of segments; while 12% showed embryonic lethality without obvious defects during dorsal closure (n=48, Fig. 6C,D and data not shown). To determine whether these phenotypes may result from defects of cell constriction at the margin, we investigated the organization of the actin cytoskeleton in *msn* and control embryos. In control embryos, actin was detected as a continuous 'cable' in marginal cells of the epidermis from stage 13 onward. Marginal cells were elongated in the movement direction and were aligned into an apparently taut row (Fig. 6E). In msn^{172} embryos, we detected intermittent breaks in the actin distribution at the margin, typically affecting groups of 2-4 cells. On average, these breaks in the actin cable were found at a frequency of two per epithelial margin at stage 13-14 (n=10). Affected cells were wider and less elongated than neighboring cells with normal actin localization (Fig. 6F).

To determine how these defects affect the closure process, we performed live imaging of embryos expressing GFP-Actin in the *engrailed* domain (see Materials and methods). In control embryos, we consistently observed perfect segment alignment along the seam where the opposing epithelial fronts have met (Fig. 6G,I; see Movie 3 in the supplementary material). In msn^{172} embryos, we observed a similar range of dorsal closure phenotypes as was detected by our cuticle preparations. In particular, we found that 30% of the embryos displayed segment misalignments during the final phase of dorsal closure (Fig. 6H,J; see Movie 4 in the supplementary material; and data not shown).

The segment misalignment defect of msn^{172} embryos was typically accompanied by unusual irregularities in the width of segments during the closure process. Some segments appeared abnormally wide, while neighboring segments became excessively constricted. This probably resulted in the failure of proper matching of opposing segments during the zippering phase of the closure process. The formation of filopodia and lamellipodia at the margin, which had been previously implicated in the control of segment matching (Jacinto et al., 2000), appeared normal in these embryos.

We therefore conclude that *Drosophila* Misshapen is required during dorsal closure for actin-based elongation and constriction of cells at the advancing epidermal margin.

Drosophila Misshapen is required specifically in marginal cells during dorsal closure

To determine whether *Drosophila* Misshapen function is specifically required in the epidermis of the embryo, we expressed a dominant-negative version of the gene [*DN-msn,* previously described by Houalla et al. (Houalla et al., 2005)] in the whole epidermis or in marginal cells alone. In both cases, analysis of the actin cytoskeleton revealed defects similar to those of msn^{172} mutants. We consistently observed breaks in the localization of actin at the margin of the epidermis (Fig. 7A,D,G). These occurred at a similar frequency to that in *msn* mutant embryos.

Furthermore, we observed abnormalities in myosin 2 localization. While control embryos showed continuous myosin 2 localization along the margin, frequent disruptions of the pattern were observed in embryos expressing *DN-msn* (Fig. 7B,E,H). These gaps in actin or myosin 2 localization correlated with reduced elongation and leading edge constriction of the affected cells (Fig. 7C,F,I). This suggests that Misshapen is required in marginal cells of the epidermis to mediate actin/myosin 2-based cel-shape changes during dorsal closure.

During dorsal closure, the amnioserosa (AS) cells change shape and constrict apically. This process is known to be driven by an apical contractile apparatus that is regulated by Drac1 and Crumbs (Harden et al., 2002). To investigate if Misshapen also plays a role in the AS, we interfered with Msn function by ectopically expressing *DN-msn* specifically in the AS cells. We found that less than 10% of the embryos (n=120) displayed cuticle phenotypes, namely with head problems that vary from an anterior hole to dorsal-anterior holes (data not shown). This phenotype suggests that Misshapen does not play a major role in amnioserosa contraction.

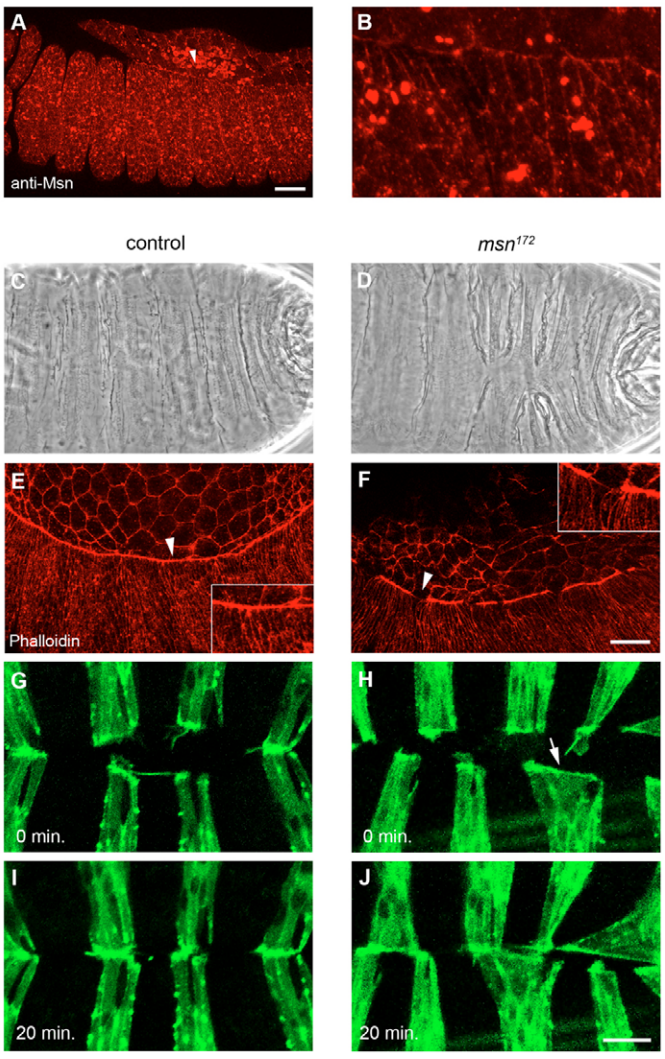

Fig. 6. *Drosophila misshapen* is required for actin-based cell constriction and segment alignment during dorsal closure. (**A**,**B**) Anti-Msn antibody staining of a stage 13 control embryo, lateral view with anterior to the left. Arrowhead in (A) indicates the region shown in a magnified view in (B). Large spots probably represent non-specific signal. (**C**,**D**) Cuticle preparations of control (C) and *msn*^{172} mutant embryos (D) after dorsal closure completion. (**E**,**F**) Phalloidin (F-actin) staining of stage 14 control (E) and *msn*^{172} mutant embryos (F). Arrowheads demarcate regions shown as insets. (**G-J**) Time-lapse analysis of the final stages of dorsal closure in control (G,I) and *msn*^{172} mutant embryos (H,J) expressing GFP-Actin in the *engrailed* domain. Embryos are shown at time points 0 min (G,H) and +20 min (I,J). Scale bars: in A, 25 μm for A,B; in F, 25 μm for E,F; in J, 10 μm for G-J.

DISCUSSION

In this study, we provide new insight into the control of coordinated cell-shape changes at the advancing margin of an epithelial sheet and suggest that conserved mechanisms mediate this process both in zebrafish and *Drosophila* (see Fig. 8 for an overview). In zebrafish, we found that the accumulation of actin and myosin 2 in the YSL is dependent on the Ste20-like kinase Msn1 and is required for cell-shape changes of marginal EVL cells during epiboly. Similarly, we found that *Drosophila* Misshapen, the ortholog of Msn1, is required for actin/myosin 2-based constriction of marginal cells of the epidermis during dorsal closure.

Previous studies have suggested that the YSL plays an important role during EVL epiboly in teleosts. Analysis of epiboly movements of *Fundulus heteroclitus* has shown that marginal EVL cells are physically linked to the YSL as they undergo changes in shape (Betchaku and Trinkaus, 1978; Keller and Trinkaus, 1987). Furthermore, both in *Fundulus* and zebrafish, the accumulation of actin within the YSL at the EVL/YSL interface has been described (Betchaku and Trinkaus, 1978; Cheng et al., 2004). Our study builds on these findings and specifically focuses on the molecular mechanism of actin recruitment in the YSL and the role of this process for cell-shape changes of the EVL.

We show that after the 50% epiboly stage, the advancement of the EVL margin towards the vegetal pole becomes in part dependent on the YSL. As in *Fundulus*, we find that the YSL in zebrafish is probably coupled to the EVL via tight junctions. Furthermore, our findings suggest that actin/myosin 2-based contraction of the YSL mediates cell-shape changes at the EVL margin. First, we demonstrated that cell elongation and leading edge constriction at the margin correlates with the accumulation of actin within the adjacent YSL. Secondly, we showed that YSL-specific inactivation of Msn1 impairs both actin/myosin 2 accumulation in the YSL and cell-shape changes of the EVL. Our data suggest that EVL epiboly is driven by YSL contraction, and implicate substrate contraction as an important mechanism to coordinate cell-shape changes of an advancing epithelial sheet.

Based on our results, we propose a specific model of how actin/myosin 2-based YSL contraction promotes EVL epiboly. Actin and myosin 2 within the YSL become recruited to the junctional complex between the EVL and YSL via a Mns1-dependent mechanism. This results in local constriction of the leading edges of marginal EVL cells. As a consequence, the overall length of the EVL margin shortens and progresses towards the vegetal pole of the spherical yolk cell (for illustration, see Fig. 8).

A central question is how the constriction of cells is coordinated at the EVL margin. The presence of a cable-like zone of actin along the closing margin of an epithelial sheet has previously invoked a purse-string mechanism (Kiehart, 1999; Williams-Masson et al., 1997). However, such a model is probably insufficient to account for the dynamic cell-shape changes of marginal EVL cells. Our findings suggest that YSL contraction may be increased at local ‘hot spots’ in the vicinity of the EVL margin, causing some marginal cells to become highly constricted, while adjacent cells widen. This results

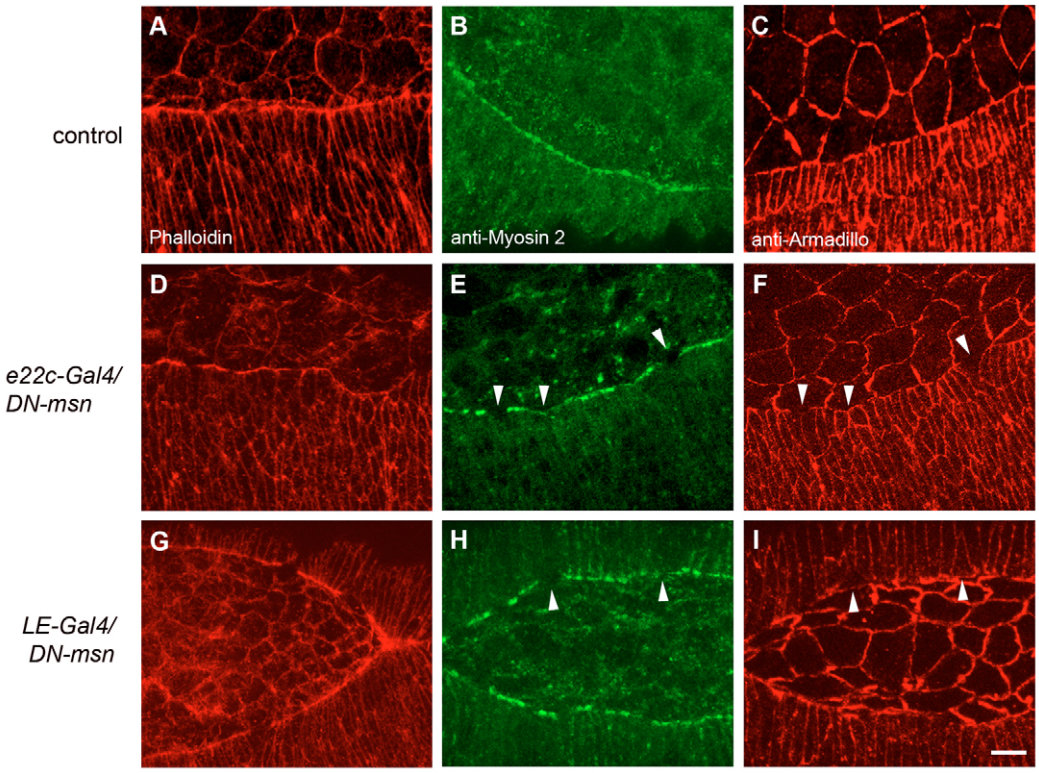

Fig. 7. *Drosophila misshapen* is required in marginal cells of the epidermis for actin and myosin 2 localization and cell constriction. Phalloidin (**A**,**D**,**G**), anti-myosin 2 (**B**,**E**,**H**) and anti-Armadillo (**C**,**F**,**I**) staining of control embryos (A-C) and embryos expressing *DN-msn* (D-I). *e22c-Gal4* (D-F) and *LE-Gal4* (G-I) were used to express *DN-msn* in the whole epidermis or in marginal cells of the epidermis, respectively. (E,F) and (H,I) show myosin 2/Armadillo co-staining. Arrowheads point at areas of disrupted myosin 2 staining correlating with abnormally wide cell shape. Scale bar: 10 μm.

in high variability of EVL cell shape observed during late stages of epiboly. Whether this is regulated autonomously within the YSL or involves signals from the EVL is currently unknown. Alternatively, contractility may be evenly distributed within the YSL, and cell constriction may occur particularly in those areas of the EVL margin that pose the least resistance. These models should be tested in future studies.

Our analysis of EVL epiboly reveals several similarities to dorsal closure in *Drosophila*. In both cases, the advancing front of an epithelial sheet becomes physically linked to the underlying substrate via junctional complexes (this study; Narasimha and Brown, 2004). Furthermore, both processes depend on actin/myosin 2-based constriction of marginal cells that is mediated by a Misshapen molecule.

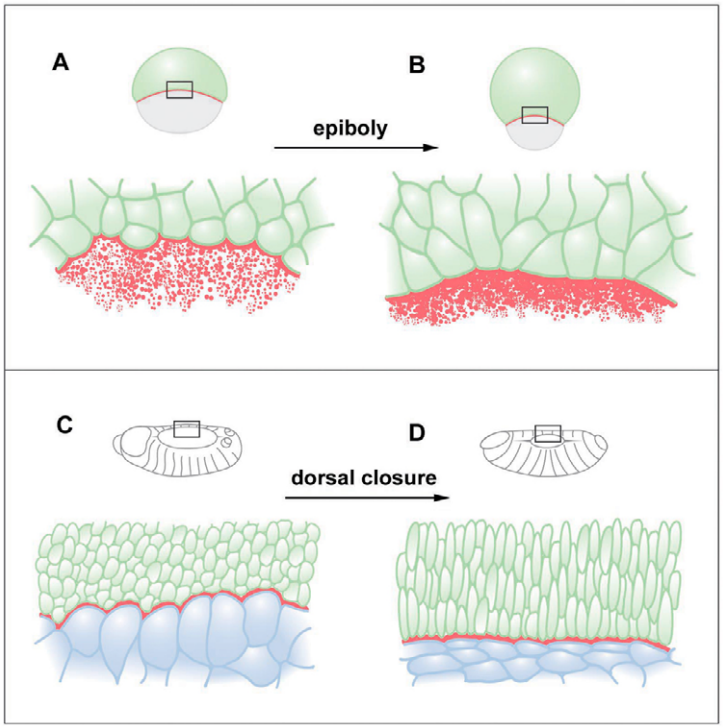

Fig. 8. Schematic representation of zebrafish epiboly and *Drosophila* dorsal closure movements. (**A**,**B**) EVL/YSL epiboly in zebrafish. At the onset of gastrulation (50% epiboly), marginal cells of the EVL (green) are oval shaped and loosely aligned at the interface between the EVL and the YSL. Actin (red) appears evenly distributed within the YSL (A). At 75% epiboly, marginal EVL cells have become increasingly elongated and aligned into a taut row. Actin has accumulated at the interface between EVL and YSL, forming an 'actin ring' within the YSL along the circumference of the embryo (B). (**C**,**D**) *Drosophila* dorsal closure. At the onset of dorsal closure, marginal cells of the lateral epidermis cells (green) are loosely aligned and are in contact with the amnioserosa cells (blue, C). Actin (red) is beginning to accumulate at the leading edges of marginal cells at this stage. With dorsal closure proceeding, marginal cells become clearly elongated and aligned as actin strongly accumulates at the leading edge of these cells (D).

Similar to EVL epiboly in zebrafish, *Drosophila* dorsal closure is probably not mediated by a simple purse-string mechanism. In embryos with impaired *misshapen* function, local disruptions of the actin/myosin 2 cable did not prevent the overall closure process. This is consistent with prior studies showing that ablation of marginal epidermal cells does not prevent completion of dorsal closure (Kiehart et al., 2000). We observed that cells lacking actin and myosin were abnormally wide, while the adjacent cells contracted excessively. This led to segment mismatches at the end of dorsal closure. Therefore, it is likely that actin/myosin 2 cable mediates coordinated cell constrictions at the margin to ensure even closure of the embryo.

In addition, our study revealed important differences between epithelial-sheet sealing in fish and flies. In zebrafish, cell-shape changes at the EVL margin are probably mediated by the underlying substrate, while in *Drosophila*, marginal cells appear to actively constrict (Jacinto et al., 2002a). We speculate that in zebrafish, actin/myosin 2-based tissue contraction along the circumference of the embryo may be most efficiently achieved in the continuous cytoplasm of the YSL. Similar observations have been made in the case of the *C. elegans* embryo, in which most cells of the outer epithelium fuse prior to the formation of contractile rings of microfilaments (Priess and Hirsh, 1986).

Another difference between EVL epiboly and dorsal closure lies in the cellular mechanism that shortens the epithelial margin during the closure process. In both cases, this involves the elimination of marginal cells. However, in *Drosophila*, cells leave the margin through the fusion of the opposing fronts of the epidermis on the anterior and posterior ends of the dorsal hole (Wood et al., 2002). In contrast, we find that in zebrafish, similar to *Fundulus*, cells along the whole circumference of the embryo are continuously removed from the margin and accommodated into rows further behind (Keller and Trinkaus, 1987). This process involves the complete elimination of the leading edges of EVL cells, probably as a result of localized contraction of the YSL.

A mechanism similar to EVL epiboly has been proposed for closure of epidermal wounds in *Drosophila*. Reduction of an epidermal wound margin involves the exclusion of marginal cells through actin-based leading-edge constriction (Wood et al., 2002). Furthermore, wound healing as well as dorsal closure of the *Drosophila* embryo require the function of an actin/myosin 2-based cell constriction. Moreover, wound closure in *Xenopus* oocytes depends on the accumulation of actin filaments and myosin 2 at the wound margin (Mandato and Bement, 2001). This suggests that further analysis of the molecular mechanism of actin/myosin 2-mediated YSL contraction will improve our understanding of the mechanisms of epithelial morphogenesis as well as wound healing.

Molecular insight into the control of actin-based YSL contraction comes from our analysis of the role of the Ste20-like kinase Msn1, which is required for actin and myosin 2 recruitment within the YSL. One candidate molecule likely to mediate Msn1 function is myosin light chain 2, as we observed decreased levels of the phosphorylated (activated) form of the protein within the YSL of *msn1* morphant embryos. Whether Msn1 functions through known activators of myosin light chain 2, such as Rho kinase, or whether it affects myosin 2 function more indirectly remains to be established. Other candidates for Msn1 effectors are suggested from studies of Misshapen in *Drosophila*. During dorsal closure, Misshapen functions upstream of the JNK pathway (Su et al., 1998; Su et al., 2000). Additionally, Misshapen has been described to interact with the actin-binding protein Bifocal during photoreceptor growth cone migration (Ruan et al., 2002; Su et al., 2000). Future studies are needed to determine which downstream targets of Misshapen-like molecules are conserved between *Drosophila* and zebrafish.

We thank B. Habermann for help with identifying the *msn1-3* genes and for performing the phylogenetic analysis. Thanks to Michaela Wilsch-Bräuninger for transmission electron microscopy work and to the laboratory of S. Eaton for help with fly work. We thank the Bloomington Stock Center, Y. Rao and J. Treisman for fly stocks, Y. Rao for the anti-Msn antibody, and D. Kiehart for the anti-myosin 2 antibody. We are grateful to Franziska Friedrich for assistance with the artwork. We thank the staff of the fish and imaging facilities at the MPI-CBG for excellent assistance. We thank C. Dahmann, A. Oates, and L. Rohde for critical reading of the manuscript. This work was supported by grants from the Emmy-Noether-Program of the DFG, the MPG and the Humboldt foundation. M.K. was supported by fellowships from the DFG and the Marie Curie Fellowship Association.

Supplementary material

Supplementary material for this article is available at
http://dev.biologists.org/cgi/content/full/133/14/2671/DC1

References

Babb, S. G., Barnett, J., Doedens, A. L., Cobb, N., Liu, Q., Sorkin, B. C., Yelick, P. C., Raymond, P. A. and Marrs, J. A. (2001). Zebrafish E-cadherin: expression during early embryogenesis and regulation during brain development. *Dev. Dyn.* **221**, 231-237.

Barth, K. A. and Wilson, S. W. (1995). Expression of zebrafish nk2.2 is influenced by sonic hedgehog/vertebrate hedgehog-1 and demarcates a zone of neuronal differentiation in the embryonic forebrain. *Development* **121**, 1755-1768.

Betchaku, T. and Trinkaus, J. P. (1978). Contact relations, surface activity, and cortical microfilaments of marginal cells of the enveloping layer and of the yolk syncytial and yolk cytoplasmic layers of fundulus before and during epiboly. *J. Exp. Zool.* **206**, 381-426.

Brand, A. H. and Perrimon, N. (1993). Targeted gene expression as a means of altering cell fates and generating dominant phenotypes. *Development* **118**, 401-415.

Cheng, J. C., Miller, A. L. and Webb, S. E. (2004). Organization and function of microfilaments during late epiboly in zebrafish embryos. *Dev. Dyn.* **231**, 313-323.

Chenna, R., Sugawara, H., Koike, T., Lopez, R., Gibson, T. J., Higgins, D. G. and Thompson, J. D. (2003). Multiple sequence alignment with the Clustal series of programs. *Nucleic Acids Res.* **31**, 3497-3500.

D'Amico, L. A. and Cooper, M. S. (2001). Morphogenetic domains in the yolk syncytial layer of axiating zebrafish embryos. *Dev. Dyn.* **222**, 611-624.

D'Atri, F. and Citi, S. (2002). Molecular complexity of vertebrate tight junctions (Review). *Mol. Membr. Biol.* **19**, 103-112.

Harden, N. (2002). Signaling pathways directing the movement and fusion of epithelial sheets: lessons from dorsal closure in Drosophila. *Differentiation* **70**, 181-203.

Harden, N., Ricos, M., Yee, K., Sanny, J., Langmann, C., Yu, H., Chia, W. and Lim, L. (2002). Drac1 and Crumbs participate in amnioserosa morphogenesis during dorsal closure in Drosophila. *J. Cell Sci.* **115**, 2119-2129.

Heasman, J. (2002). Morpholino oligos: making sense of antisense? *Dev. Biol.* **243**, 209-214.

Houalla, T., Hien Vuong, D., Ruan, W., Suter, B. and Rao, Y. (2005). The Ste20-like kinase misshapen functions together with Bicaudal-D and dynein in driving nuclear migration in the developing drosophila eye. *Mech. Dev.* **122**, 97-108.

Jacinto, A., Wood, W., Balayo, T., Turmaine, M., Martinez-Arias, A. and Martin, P. (2000). Dynamic actin-based epithelial adhesion and cell matching during Drosophila dorsal closure. *Curr. Biol.* **10**, 1420-1426.

Jacinto, A., Wood, W., Woolner, S., Hiley, C., Turner, L., Wilson, C., Martinez-Arias, A. and Martin, P. (2002a). Dynamic analysis of actin cable function during Drosophila dorsal closure. *Curr. Biol.* **12**, 1245-1250.

Jacinto, A., Woolner, S. and Martin, P. (2002b). Dynamic analysis of dorsal closure in Drosophila: from genetics to cell biology. *Dev. Cell* **3**, 9-19.

Kaltschmidt, J. A., Lawrence, N., Morel, V., Balayo, T., Fernandez, B. G., Pelissier, A., Jacinto, A. and Martinez Arias, A. (2002). Planar polarity and actin dynamics in the epidermis of Drosophila. *Nat. Cell Biol.* **4**, 937-944.

Kane, D. and Adams, R. (2002). Life at the edge: epiboly and involution in the zebrafish. *Results Probl. Cell Differ.* **40**, 117-135.

Kane, D. A., Hammerschmidt, M., Mullins, M. C., Maischein, H. M., Brand, M., van Eeden, F. J., Furutani-Seiki, M., Granato, M., Haffter, P., Heisenberg, C. P. et al. (1996). The zebrafish epiboly mutants. *Development* **123**, 47-55.

Kane, D. A., McFarland, K. N. and Warga, R. M. (2005). Mutations in half baked/E-cadherin block cell behaviors that are necessary for teleost epiboly. *Development* **132**, 1105-1116.

Keller, R. E. and Trinkaus, J. P. (1987). Rearrangement of enveloping layer cells without disruption of the epithelial permeability barrier as a factor in Fundulus epiboly. *Dev. Biol.* **120**, 12-24.
Kiehart, D. P. (1999). Wound healing: The power of the purse string. *Curr. Biol.* **9**, R602-R605.
Kiehart, D. P. and Feghali, R. (1986). Cytoplasmic myosin from Drosophila melanogaster. *J. Cell Biol.* **103**, 1517-1525.
Kiehart, D. P., Galbraith, C. G., Edwards, K. A., Rickoll, W. L. and Montague, R. A. (2000). Multiple forces contribute to cell sheet morphogenesis for dorsal closure in Drosophila. *J. Cell Biol.* **149**, 471-490.
Kimmel, C. B., Ballard, W. W., Kimmel, S. R., Ullmann, B. and Schilling, T. F. (1995). Stages of embryonic development of the zebrafish. *Dev. Dyn.* **203**, 253-310.
Mandato, C. A. and Bement, W. M. (2001). Contraction and polymerization cooperate to assemble and close actomyosin rings around Xenopus oocyte wounds. *J. Cell Biol.* **154**, 785-797.
Martin, P. and Parkhurst, S. M. (2004). Parallels between tissue repair and embryo morphogenesis. *Development* **131**, 3021-3034.
Martinez-Arias, A. (1993). Development and patterning of the larval epidermis of Drosophila. In *The Development of Drosophila melanogaster* (ed. A. Martinez-Arias and M. Bate), pp. 517-607. Cold Spring Harbor: Cold Spring Harbor Laboratory Press.
Montero, J. A., Carvalho, L., Wilsch-Brauninger, M., Kilian, B., Mustafa, C. and Heisenberg, C. P. (2005). Shield formation at the onset of zebrafish gastrulation. *Development* **132**, 1187-1918.
Nagafuchi, A. (2001). Molecular architecture of adherens junctions. *Curr. Opin. Cell Biol.* **13**, 600-603.
Narasimha, M. and Brown, N. H. (2004). Novel functions for integrins in epithelial morphogenesis. *Curr. Biol.* **14**, 381-385.
Perriere, G. and Gouy, M. (1996). WWW-query: an on-line retrieval system for biological sequence banks. *Biochimie* **78**, 364-369.
Priess, J. R. and Hirsh, D. I. (1986). Caenorhabditis elegans morphogenesis: the role of the cytoskeleton in elongation of the embryo. *Dev. Biol.* **117**, 156-173.
Ruan, W., Pang, P. and Rao, Y. (1999). The SH2/SH3 adaptor protein dock interacts with the Ste20-like kinase misshapen in controlling growth cone motility. *Neuron* **24**, 595-605.
Ruan, W., Long, H., Vuong, D. H. and Rao, Y. (2002). Bifocal is a downstream target of the Ste20-like serine/threonine kinase misshapen in regulating photoreceptor growth cone targeting in Drosophila. *Neuron* **36**, 831-842.
Straight, A. F., Cheung, A., Limouze, J., Chen, I., Westwood, N. J., Sellers, J. R. and Mitchison, T. J. (2003). Dissecting temporal and spatial control of cytokinesis with a myosin II Inhibitor. *Science* **299**, 1743-1747.
Su, Y. C., Treisman, J. E. and Skolnik, E. Y. (1998). The Drosophila Ste20-related kinase misshapen is required for embryonic dorsal closure and acts through a JNK MAPK module on an evolutionarily conserved signaling pathway. *Genes Dev.* **12**, 2371-2380.
Su, Y. C., Maurel-Zaffran, C., Treisman, J. E. and Skolnik, E. Y. (2000). The Ste20 kinase misshapen regulates both photoreceptor axon targeting and dorsal closure, acting downstream of distinct signals. *Mol. Cell. Biol.* **20**, 4736-4744.
Treisman, J. E., Ito, N. and Rubin, G. M. (1997). misshapen encodes a protein kinase involved in cell shape control in Drosophila. *Gene* **186**, 119-125.
Trinh, L. A. and Stainier, D. Y. (2004). Fibronectin regulates epithelial organization during myocardial migration in zebrafish. *Dev. Cell* **6**, 371-382.
Williams-Masson, E. M., Malik, A. N. and Hardin, J. (1997). An actin-mediated two-step mechanism is required for ventral enclosure of the C. elegans hypodermis. *Development* **124**, 2889-2901.
Wood, W., Jacinto, A., Grose, R., Woolner, S., Gale, J., Wilson, C. and Martin, P. (2002). Wound healing recapitulates morphogenesis in Drosophila embryos. *Nat. Cell Biol.* **4**, 907-912.
Xue, Y., Wang, X., Li, Z., Gotoh, N., Chapman, D. and Skolnik, E. Y. (2001). Mesodermal patterning defect in mice lacking the Ste20 NCK interacting kinase (NIK). *Development* **128**, 1559-1572.
Young, P. E., Richman, A. M., Ketchum, A. S. and Kiehart, D. P. (1993). Morphogenesis in Drosophila requires nonmuscle myosin heavy chain function. *Genes Dev.* **7**, 29-41.